

# 1 **PySWR- A Python Code for Fitting Soil Water Retention Functions**

2 **Sama S. Memari<sup>1</sup>, T. Prabhakar Clement<sup>1</sup>**

3 <sup>1</sup>Department of Civil, Construction and Environmental Engineering, University of Alabama,  
4 Tuscaloosa, Alabama, USA.

5 **Abstract:** Soil water retention (SWR) function is an important model that provides an  
6 empirical relationship between soil moisture and capillary pressure. We present a simple Python  
7 tool for fitting different types of SWR functions to laboratory-measured soil moisture data. Three  
8 different optimization methods including the Levenberg-Marquardt (LM) method, Trust Region  
9 Reflective (TR) method, and Dog Box (DB) method are considered. We used all three methods  
10 to fit the van Genuchten (VG) and Brooks and Corey (BC) models to ten soil moisture datasets.  
11 Our results show that the TR method, which allows the user to search for optimal parameter  
12 values within a constrained region, is the best approach for fitting these models. We developed a  
13 new graphical procedure for evaluating the guesstimates and bounds for different SWR model  
14 parameters. Overall, the TR method available in Python, together with the proposed graphical  
15 procedure, is an excellent approach for fitting both VG and BC models to soil moisture data.

16 **Keywords:** soil water retention function; van Genuchten model; Brooks and Corey model;  
17 parameter estimation; curve fitting; Python

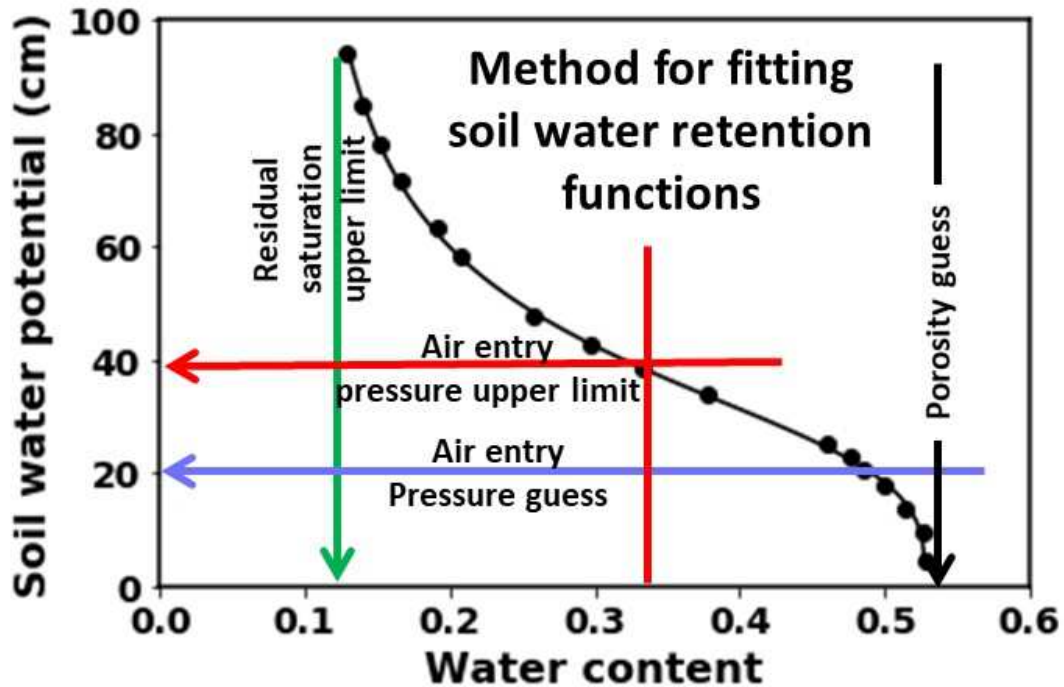
## 18 **Author Contribution**

19 SSM developed the code, completed simulations, and co-wrote the manuscript.

20 TPC developed ideas, debugged the code, and co-wrote the manuscript.

21

22 Graphical Abstract



23

24 **Highlights**

- 25 • A Python code for fitting soil water retention models to experimental data is provided
- 26 • PySWR can fit both van Genuchten and Brooks and Corey water retention models
- 27 • PySWR supports two constrained and one unconstrained non-linear fitting methods
- 28 • A graphical approach has been developed to provide good initial guesses and parameter
- 29 bounds
- 30 • Trust region reflective method is the best approach for fitting soil water retention models

31

32

33

34

## 35 **1. Introduction**

36 A soil water retention (SWR) function is an empirical model that describes the relationship  
37 between volumetric water content and soil matric pressure head. This empirical relationship is an  
38 important function used in computer simulation tools that are employed for solving practical  
39 problems in hydrology and geotechnical engineering fields (Clement et al., 1994; Clement et al.,  
40 1996; Tuller et al., 2004; Malaya and Sreedeeep, 2012). SWR function characterizes the ability of  
41 the soil to store and release water, and is also used for estimating several unsaturated soil  
42 properties that are used in hydroclimatic and hydrologic models (Mohanty and Zhu, 2007; Shin  
43 et al., 2012). Therefore, both laboratory and field approaches for developing SWR functions  
44 have received widespread attention in recent years (Schindler et al., 2012; Masaoka and Kosugi,  
45 2018; Roy et al., 2018; Shokrana and Ghane, 2020).

46 In the published literature, several analytical models have been suggested for modeling SWR  
47 functions and this includes the Brooks and Corey (BC) model (Brooks and Corey, 1964),  
48 Fredlund-Xing model (Fredlund and Xing, 1994), Gardner model (Gardner, 1958), Campbell  
49 model (Campbell, 1974), and van Genuchten (VG) model (Van Genuchten, 1980), to name a  
50 few. Among these models, VG and BC models are the most widely used functions. The  
51 parameters in these models are typically identified by fitting these model functions to measured  
52 soil moisture data using a nonlinear curve fitting method. Both field and laboratory data have  
53 been used in such fitting exercises. For field problems, researchers have employed various types  
54 of inverse modeling approaches that utilize unsaturated flow codes, such as HYDRUS, to fit  
55 field-observed soil moisture data (Simunek and Van Genuchten, 1999; Wang et al., 2016). Lai  
56 and Ren (2016) combined HYDRUS-1D and PEST (a general-purpose parameter estimation  
57 software) (Doherty et al., 2010) to determine the effective soil hydraulic parameters at a field

58 site. PEST employs a nonlinear parameter estimation algorithm known as the Gauss-Marquardt-  
59 Levenberg method. The results of this study indicated that there are no unique set of average soil  
60 properties for fitting water content values measured at a heterogeneous field site. Ket et al.  
61 (2018) used a capacitance probe and a dielectric water potential sensor to measure soil water  
62 content and water potential, respectively, at a field site. They used HYDRUS-1D to fit the in situ  
63 data to indirectly estimate the values of VG parameters for different types of soils. Nascimento et  
64 al. (2018) used multiple instruments to measure the values of matric potential and soil moisture  
65 levels in a field experiment and then used HYDRUS-1D to estimate the VG model parameters.  
66 They concluded that HYDRUS-1D was able to estimate the VG model parameters well, and the  
67 values were found to be consistent with laboratory estimates.

68 For fitting SWR data, researchers have employed different types of nonlinear least square (NLS)  
69 algorithms and heuristic search (HS) methods. Several numerical codes have been developed for  
70 solving this curve-fitting problem. One of the codes that use an NLS method is the RETC code,  
71 and it is used widely for fitting different types of SWR models (Van Genuchten and Yates,  
72 1991). Omuto and Gumbe (2009) used the Gauss-Newton algorithm available in R for fitting soil  
73 hydraulic properties used in infiltration and water retention models. Kumar et al. (2020)  
74 developed a software tool for fitting BC, VG, and modified-VG models using the Levenberg-  
75 Marquardt NLS routine available within the SPSS statistical software package. One of the  
76 limitations of using NLS algorithms is that the final solution would depend on the quality of the  
77 initial guesses and therefore the estimated model parameters might not be the unique global  
78 optimal values. HS algorithms, which are independent of initial conditions, offer a more robust  
79 alternative for estimating optimal SWR parameters (Chen et al., 2016). However, HS methods  
80 have other numerical parameters that need to be adjusted a priori to obtain valid solutions. This

81 requirement could affect the final output, and also the process of adjusting these parameters can  
82 be computationally inefficient (Li et al., 2018; Luo et al., 2018). To avoid the issues related to  
83 algorithm-specific parameter adjustments, Zhang et al. (2018) employed a novel salp swarm  
84 algorithm (SSA) and used it to fit SWR functions. They also compared the performance of the  
85 SSA method with three other methods for fitting SWR functions. Their results indicated that  
86 SSA can yield better results. Recently, Guellouz et al. (2020) presented a study where they used  
87 the bound optimization by quadratic approximation (BOBYQA) approach to fit a finite  
88 difference model, which is based on the Richards' equation, to simulate a field experiment. They  
89 analyzed a drainage experiment conducted at field site in Southwestern Tunisia to estimate the  
90 VG parameters for the site.

91 The tools reviewed above require complex computer programs for fitting SWR models, and also  
92 all these programs have some computational limitations. The objective of this study is to develop  
93 a simple, yet robust, computer tool for fitting VG and BC models to laboratory-measured soil  
94 moisture data. The Python module SciPy offers several computationally efficient solvers for  
95 fitting a nonlinear function to experimental data. In this study, we developed a Python code,  
96 namely PySWR, that employs SciPy for fitting SWR functions. We evaluated the code  
97 performance by fitting VG and BC functions to ten experimental datasets available in the  
98 literature.

## 99 **2. Methods**

### 100 **2.1. van Genuchten SWR model**

101 The VG model (Van Genuchten, 1980) is the most widely used SWR model since it is a smooth  
102 mathematical function without any discontinuities. This model has been used to describe a broad

103 range of disturbed and undisturbed soils. The model is an explicit analytical function that  
 104 describes the volumetric water content  $\theta$  as a function of capillary pressure as:

$$\frac{\theta - \theta_r}{\theta_s - \theta_r} = [1 + (\alpha|h|^n)]^{-m} \quad (1)$$

105 where  $\theta$  is the volumetric water content ( $\text{cm}^3/\text{cm}^3$ );  $\theta_r$  is the residual water content ( $\text{cm}^3/\text{cm}^3$ ),  $\theta_s$   
 106 is the saturated water content ( $\text{cm}^3/\text{cm}^3$ );  $h$  is the capillary pressure head (cm) which is a negative  
 107 number;  $\alpha$  ( $\text{cm}^{-1}$ ) is a parameter that is related to the inverse of the air entry pressure;  $n$  is a  
 108 parameter that is related to the shape of the pore size distribution (Wise, 1992; Wang et al.,  
 109 2017); and  $m$  is typically related to the value of  $n$  via the expression:  $m=1-1/n$ . The VG model is  
 110 a two-parameter model and its shape is controlled by the values of  $\alpha$  and  $n$ . The model parameter  
 111  $\alpha$  is proportional to the inverse air entry value and its value can range from about  $0.005 \text{ cm}^{-1}$  for  
 112 fine clays to about  $1 \text{ cm}^{-1}$  for coarse sand. The dimensionless value of  $n$  controls the shape of the  
 113 drainage pattern and its value can be as high as 10 for uniform soils (such as well-graded sand)  
 114 that will have sharp drainage pattern, and it can be as low as 1.1 for heterogeneous soils (such as  
 115 silty clay) that will have diffused drainage pattern (Wise et al., 1994; Cornelis et al., 2005).

## 116 2.2. Brooks and Corey SWR model

117 Another popular empirical function used for modeling SWR data is the BC model (Brooks and  
 118 Corey, 1964). This model relates soil moisture value with capillary pressure using the following  
 119 equations:

$$\theta = \begin{cases} \theta_r + (\theta_s - \theta_r)|\beta h|^{-\lambda} & (h < -1/\beta) \\ \theta_s & (h \geq -1/\beta) \end{cases} \quad (2)$$

120 Where  $\beta$  ( $\text{cm}^{-1}$ ) is the inverse of air entry value (or bubbling pressure)  $h_b$  (cm),  $\lambda$  is a pore size  
 121 distribution index and other terms are defined above. The BC model is a two-parameter model.  
 122 Unlike the VG model, the BC model is not a smooth function since it has a discontinuity close to

123 the air entry value, a capillary pressure below which the soil is assumed to be fully saturated.  
124 Note, the BC model parameter  $\lambda$  is similar to the VG parameter  $\alpha$ . Typically, the value of  
125 bubbling pressure  $h_b$  (cm) for clay soils is high and can range from about 100 to 200 cm; for  
126 sand, it is relatively small and can range from 1 to 10 cm. The pore size distribution index  $\lambda$  is  
127 related to the VG parameter  $n$ . Lenhard et al. (1989) provided the following analytical expression  
128 that approximately relates  $\lambda$  to the value of  $n$ :

$$\lambda = \frac{m}{1-m} \left(1 - 0.5^{\frac{1}{m}}\right) \quad (3)$$

129 where  $m=1-1/n$ . Therefore, similar to  $n$ , the parameter  $\lambda$  is also related to the shape of the pore-  
130 size distribution. If the pores are relatively uniform the soil will have a sharp drainage pattern  
131 (since all the pores will drain at a similar capillary pressure). On the other hand, if the pore size  
132 distribution is wide then the soil will have a smooth drainage pattern. The typical value of  $\lambda$  can  
133 range from 5 for uniform sand to about 0.1 for highly heterogeneous silty-sandy clay soils  
134 (Fuentes et al., 1992; Stankovich and Lockington, 1995).

### 135 **2.3. Fitting SWR functions to experimental data using non-linear optimization methods**

136 The problem of fitting a SWR model to an experimental dataset can be formulated as a least-  
137 squares nonlinear optimization problem, where the model parameters are obtained using a curve-  
138 fitting algorithm. Nonlinear curve fitting is a process of minimizing the error between data and  
139 model predictions by varying the model parameters over a range of possible values. Here we will  
140 employ the following three curved fitting algorithms that are available in the Python SciPy  
141 module: Levenberg-Marquardt (LM) algorithm (Levenberg, 1944; Marquardt, 1963), Trust  
142 Region Reflective (TR) algorithm (Fletcher, 1980; Sorensen, 1982), and Dogleg algorithm with a  
143 rectangular trust region (DB) (Voglis and Lagaris, 2004). In the past, others have used the LM

144 algorithm, which is an unconstrained optimization method, for fitting SWR models (Van  
145 Genuchten and Yates, 1991; Zhang et al., 2018). However, the LM method can be inefficient for  
146 highly nonlinear problems. For these cases, TR or DB could be a better alternative since they  
147 allow the model parameter values to be constrained using a set of user-specified bounds. For  
148 example, Le et al. (2017) used a new numerical method to estimate several parameters of a non-  
149 linear elastic visco-plastic (EVP) creep model for soft soils. Their numerical approach employed  
150 the TR algorithm to fit EVP model parameters. This study also explored some of the limitations  
151 of the TR algorithm. As summarized in this study, the TR method approximates the objective  
152 function  $f(x)$  with a quadratic function  $q(s)$  that reflects the behavior of function  $f(x)$  in a  
153 neighborhood  $N$ , which is called the trust-region around a point  $x_k$ . The model is “trusted” within  
154 a limited region around this current point defined by the trust-region sub-problem. This approach  
155 can limit the length of the step as one move from  $x_k$  to  $x_{k+1}$ . Therefore, the method can be  
156 inefficient for very large constrained optimization problems. However, the fitting problem that  
157 considered in this study only had two unknown parameters and we did not encounter any  
158 computational inefficiencies in all our simulations.

#### 159 **2.4. Experimental data for testing the performance of various curve fitting methods**

160 Ten soil moisture datasets are analyzed in this study. Four of these datasets are taken from Van  
161 Genuchten and Yates (1991) study, where these data were used to test the performance of the  
162 RETC code for fitting both VG and BC functions. These four RETC soils are labeled as Weld  
163 silty clay loam (Jensen and Hanks, 1967), Touchet silt loam (King, 1965), G.E. No. 2 sand  
164 (King, 1965), and Sarpy loam (Hanks and Bowers, 1962) (See Table S1 in Supplementary  
165 Material for more details about this sample dataset).



166 Six other datasets were taken from the UNsaturated SOil hydraulic DAtabase (UNSODA). The  
167 UNSODA is a public domain resource and it provides a wide range of data for several soils. In  
168 this study, we used the UNSODA V2.0 available at this website: <https://data.nal.usda.gov/>. These  
169 soil data are presented in a format that can be directly accessed through Microsoft Access-97  
170 (Schaap et al., 2015). The six datasets selected to study include sandy, silty, loamy, and clayey  
171 type soils collected at different field sites (See Table S2 in Supplementary Material for more  
172 details about this sample dataset).

### 173 **3.0. Results and Discussion**

174 The basic source code for the PySWR Python script is available at Github  
175 (<https://github.com/tpclement/PySWR>; see Appendix A for more details). PySWR is a relatively  
176 short code that offers three powerful options (LM, TR, and DB algorithms) for fitting both VG  
177 and BC models to soil moisture data. The code also supports data visualization and error analysis  
178 tools. The experiment data are input to the code in a two-column format (pressure head vs. soil  
179 moisture) using a standard EXCEL CSV format (See Table S3 in Supplementary Material for a  
180 sample dataset).

#### 181 **3.1 *Van Genuchten model results***

182 To understand the relative performance of LM, TR, and DB algorithms for fitting the VG model,  
183 we first fitted the model to one of the RETC soils (Touchet silt loam (King, 1965)) using all  
184 three optimization methods. A standard set of initial guess values for the model parameters,  
185 provided by Zhang et al. (2018), was used; these values are summarized in Table 1. The table  
186 also provides a generic set of lower and upper bounds given by Zhang et al. (2018); these values

187 were employed when running TR and DB methods. The table also provides a generic set of  
 188 initial guesses as well as the lower and upper bounds for all BC model parameters.

189 **Table 1.** The initial guesses and lower and upper bounds used  
 190 for various model parameters.  
 191

Parameters	$\theta_r$	$\theta_s$	VG model		BC model	
			n	$\alpha$ (cm <sup>-1</sup> )	$\lambda$	$\square$ (cm <sup>-1</sup> )
Initial guess	0.05	0.4	1	1	0.1	1
Lower bound	0	0	1	0	0	0
Upper bound	1	1	100	100	100	100

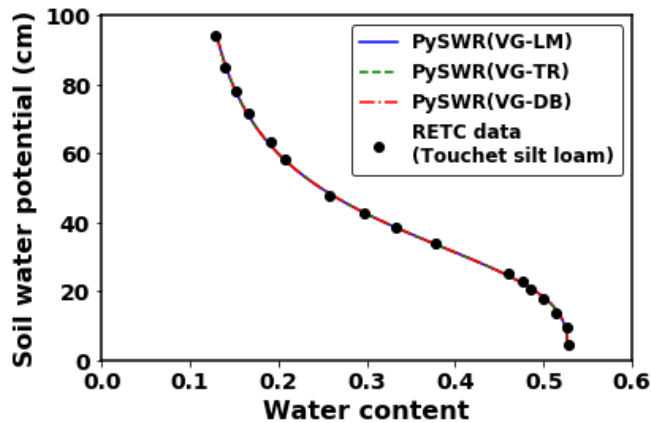
194 The values of VG model parameters estimated by PySWR, literature-derived RETC estimates  
 195 (Van Genuchten and Yates, 1991), and the computational time taken by all three fitting  
 196 algorithms are summarized in Table 2. Figure 1 compares experimental data with the fitted  
 197 model results (note absolute values of soil water potential are plotted in all the figures). The  
 198 results show that it is almost impossible to distinguish the difference between the curves fitted  
 199 using the three methods. The data presented in Table 2 also show that all three methods  
 200 estimated identical parameter values. The code was run on a standard windows-based computer  
 201 with Intel(R) Core(TM) i5 processor and 8.00 GB memory and all three methods took a fraction  
 202 of a second to converge.

203 **Table 2.** The values of van Genuchten model parameters for Touchet silt loam (King, 1965)  
 204 estimated using the three fitting methods.

Method	$\theta_r$	$\theta_s$	n	$\alpha$ (cm <sup>-1</sup> )	Comp time (s)
LM	0.092±(0.004)	0.527±(0.001)	3.5±(0.07)	0.0270±(0.0001)	0.092
TR	0.092±(0.004)	0.527±(0.001)	3.5±(0.07)	0.0270±(0.0001)	0.102
DB	0.092±(0.004)	0.527±(0.001)	3.5±(0.07)	0.0270±(0.0001)	0.130
RETC Code	0.102	0.526	3.5	0.027	---

205

206



207

208 **Figure 1.** van Genuchten soil water retention function for Touchet silt loam (King, 1965) fitted  
 209 using the three methods.

210

211 The Python tool can also compute the uncertainty (or error) in the estimated values of model  
 212 parameters (which are the square root of the diagonal entries of the covariance matrix output by  
 213 the fitting routine). The standard error values for various model parameters estimated by the  
 214 three fitting methods are summarized in Table 2. Interestingly, the uncertainly estimates  
 215 computed using all three optimization algorithms are identical.

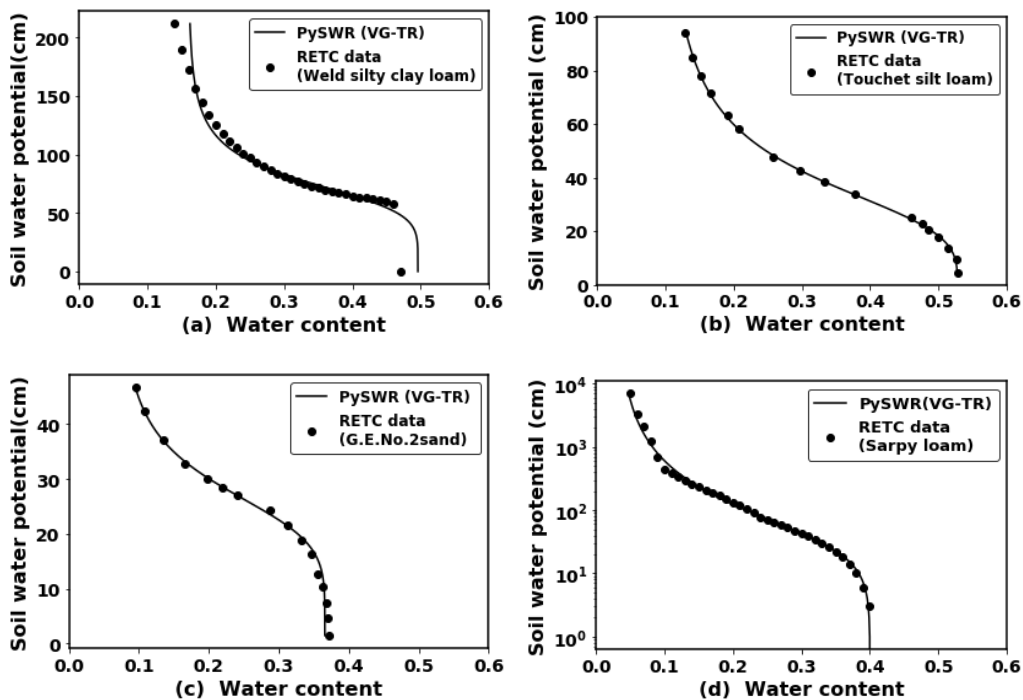
216 Since the parameter values estimated by all three fitting methods were identical, for other RETC  
 217 soils we only report the values estimated using the TR method. We selected the TR method since  
 218 it is computationally a bit more efficient than the DB method (see Table 2), and it also allowed  
 219 the user to constrain the parameter space based on our prior knowledge of the parameter values.  
 220 As illustrated in our later examples, constraining the parameters can have several advantages.

221 Figure 2 presents the model fits for all four RETC soils. In Table 3 the parameter values  
 222 estimated by PySWR are compared against the values reported in the RETC manual. The figures  
 223 show that the TR method was able to fit the VG model well for all four RETC datasets. Also, the  
 224 data shown in the table indicate that the fitted parameter values are close to the values estimated

225 using the RETC code. The sum of square error (SSE) value reported in the table was calculated  
 226 as the metric to evaluate the difference between the measured and the estimated water content  
 227 values. The SSE is defined as follows:

$$SSE = \sum_{i=1}^N (\theta_i^{obs} - \theta_i^{est})^2 \quad (4)$$

228 Where  $\theta_i^{obs}$  is the observed data, while  $\theta_i^{est}$  is the estimated value and N is the total number of  
 229 measurements in each soil sample. The SSE data show that the TR method provided better fits  
 230 for most of the soils.



231

232

233 **Figure 2.** van Genuchten model fits for the four RETC soils fitted using the TR method: (a)  
 234 Weld silty clay loam (Jensen and Hanks, 1967) (b) Touchet silt loam (King, 1965) (c) G.E.No.2  
 235 sand (King, 1965) (d) Sarpy loam (Hanks and Bowers, 1962).

236

237

238 **Table 3** The values of van Genuchten model parameters estimated using the TR method for the  
 239 four RETC soils.

Soil type	Method	$\theta_r$	$\theta_s$	n	$\alpha$ (cm <sup>-1</sup> )	SSE (10 <sup>-3</sup> )
Weld silty clay loam (Jensen and Hanks, 1967)	TR	0.159±(0.006)	0.49±(0.01)	5.4±(0.3)	0.0136±(0.0002)	4.85
	RETC code	0.15	0.49	5.4	0.0136	4.87
Touchet silt loam (King, 1965)	TR	0.092±(0.004)	0.527±(0.001)	3.50±(0.07)	0.0270±(0.0001)	0.10
	RETC code	0.102	0.526	3.59	0.027	0.17
G. E. No.2 sand (King, 1965)	TR	0.069±(0.007)	0.365±(0.002)	5.4±(0.2)	0.0367±(0.0003)	0.23
	RETC code	0.057	0.367	5.0	0.0364	0.34
Sarpy loam (Hanks and Bowers, 1962)	TR	0.031±(0.005)	0.400±(0.002)	1.59±(0.02)	0.027±(0.001)	0.98
	RETC code	0.032	0.400	1.60	0.027	0.99

240

### 241 *3.2 Brooks and Corey model results*

242 Similar to the previous section, we used the generic initial guesses and the generic upper and  
 243 lower bounds provided in Table 1 to fit the BC model to the Touchet silt loam data using all  
 244 three fitting methods. The model parameter values estimated for Touchet silt loam are  
 245 summarized in Table 4. The table also provides the optimal values of BC parameters estimated  
 246 using the RETC code (Van Genuchten and Yates, 1991). These results show that the LM method  
 247 failed to evaluate good estimates for  $\lambda$ , and even provided an unrealistic negative value for the  
 248 residual water content. On the other hand, both TR and DB estimated more realistic BC model  
 249 parameter values. We repeated the fitting exercise for several other soil datasets (details of these  
 250 soils are discussed in later sections), and for many of these cases, the LM method either failed to  
 251 converge or estimated unrealistic values. Furthermore, our test simulations indicated that  
 252 providing better initial guess values and also constraining the parameter values within a narrow  
 253 range (rather than the broad range provided in Table 1) yielded better results when using the TR

254 and DB methods. Therefore, in the following section, we propose a practical approach for  
 255 estimating initial guess and upper-and-lower bounds values for various model parameters by  
 256 graphically analyzing the experimental data.

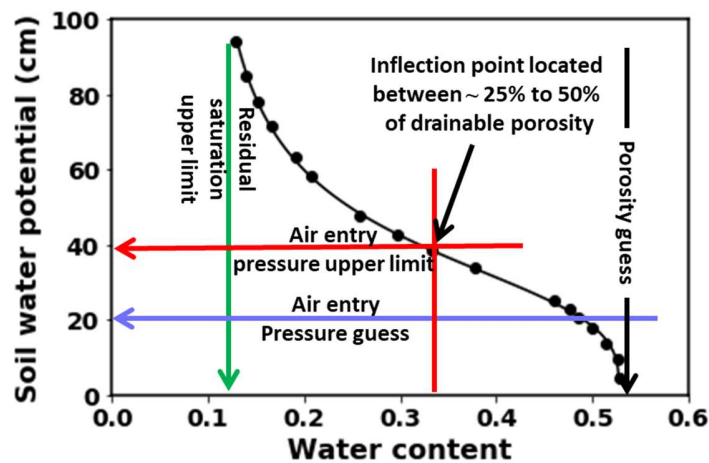
257 **Table 4.** The values of Brooks and Corey model parameters for  
 258 Touchet silt loam (King, 1965) estimated using the three fitting methods.  
 259

Method	$\theta_r$	$\theta_s$	$\lambda$	$\alpha$ (cm <sup>-1</sup> )
LM	-0.67	0.51	0.26	0.05
TR	0	0.510±(0.007)	0.9±(0.2)	0.045±(1e-3)
DB	0	0.510±(0.007)	0.9±(0.2)	0.045±(1e-3)
RETC code	0.018	0.499	1.1	0.037

260  
 261 Figure 3 summarizes the details of the proposed graphical approach for evaluating better initial  
 262 guesses and parameter bounds. We present the data analysis steps for the Touchet silt loam  
 263 (King, 1965) dataset to demonstrate this intuitive graphical approach. As a first step, we  
 264 estimated the initial guess value for porosity by drawing a vertical line connecting a few data  
 265 points which are close to maximum water content. As shown in Figure 3, this line (black line)  
 266 intersected the x-axis at the moisture content value of about 0.52, which will be our initial guess  
 267 for the value of saturated water content (or porosity). We then perturbed this porosity value by  
 268 about 25% on either side to estimate the lower and upper bounds for porosity as 0.40 to 0.65,  
 269 respectively.

270 To estimate the initial guess value of the air entry pressure, we evaluated a transition point where  
 271 the soil started to drain sharply (i.e., the water content started to decrease sharply from the  
 272 maximum saturation level) and a horizontal line (blue-line) was drawn through this point and the  
 273 line intersected the y-axis at the capillary pressure value of about 20 cm, which was assumed to  
 274 be the guess value of the air entry pressure. To estimate the upper bound for the air entry  
 275 pressure, we identified an inflection point that normally occurs somewhere between 25% to 50%

276 of the drainable porosity (this range is an estimate based on our experience of analyzing multiple  
 277 SWR datasets including the ten datasets presented in this study). For the loam soil, the inflection  
 278 point is located close to the water content value of 0.35 (as marked by the vertical red line  
 279 without an arrow). We then drew a horizontal line (red line) going through the inflection point  
 280 and estimated the upper bound for the air entry pressure as 40 cm for the loam soil (See Figure  
 281 3). The lower bound for the air entry pressure was always assumed to be 1 cm (which is an  
 282 extremely low value, typically observed for coarse sands).



283

284 **Figure 3.** Graphic approach for estimating the initial guess values, and lower and upper bounds  
 285 for VG and BC model parameters.

286

287 To estimate the value of the upper bound of the residual saturation, a vertical line (green line)  
 288 was drawn that connected a few data points that have very low water content values. This line  
 289 intersected the x-axis at the water content value of 0.12, and this value was assumed as the upper  
 290 bound for residual saturation. Since the value of residual water content will always be tending  
 291 towards zero, we assumed zero as the lower bound for all soils. However, if a better value of  
 292 residual saturation is available, the user can always use that value as the lower bound. The best

293 initial guess for residual saturation was then estimated as the midpoint between the upper and  
 294 lower bound values; for the loam soil this value is estimated to be 0.06.

295 The typical value of  $\lambda$  would range from 5 for uniform material (such as uniform sand), to a low  
 296 value of about 0.1 for highly heterogeneous silty-clay materials. The initial value for  $\lambda$  was  
 297 always assumed to be 1, which is close to the logarithmic midpoint of the range of possible  $\lambda$   
 298 values. We analyzed all four RETC soils using the proposed graphical approach and estimated  
 299 initial guesses and upper and lower bounds, and the data are summarized in Table 5.

300 **Table 5.** Initial guess values and lower and upper bounds for Brooks and Corey parameters  
 301 estimated using the proposed graphical approach for the four RETC soils (the values are  
 302 organized as  $\theta_r, \theta_s, \lambda, \alpha$  (cm<sup>-1</sup>))  
 303

Soil type	Initial guess	Lower bound	Upper bound
Weld silty clay loam (Jensen and Hanks, 1967)	0.07, 0.47, 1.0, 0.016	0, 0.35, 0.1, 1	0.14, 0.58, 5, 0.012
Toucher silt loam (King 1965)	0.06, 0.52, 1.0, 0.055	0, 0.39, 0.1, 1	0.12, 0.65, 5, 0.025
G. E. No.2 sand (King, 1965)	0.045, 0.37, 1.0, 0.083	0, 0.28, 0.1, 1	0.09, 0.46, 5, 0.04
Sarpy loam (Hanks and Bowers, 1962)	0.035, 0.40, 1.0, 0.1	0, 0.3, 0.1, 1	0.07, 0.5, 5, 0.0025

304

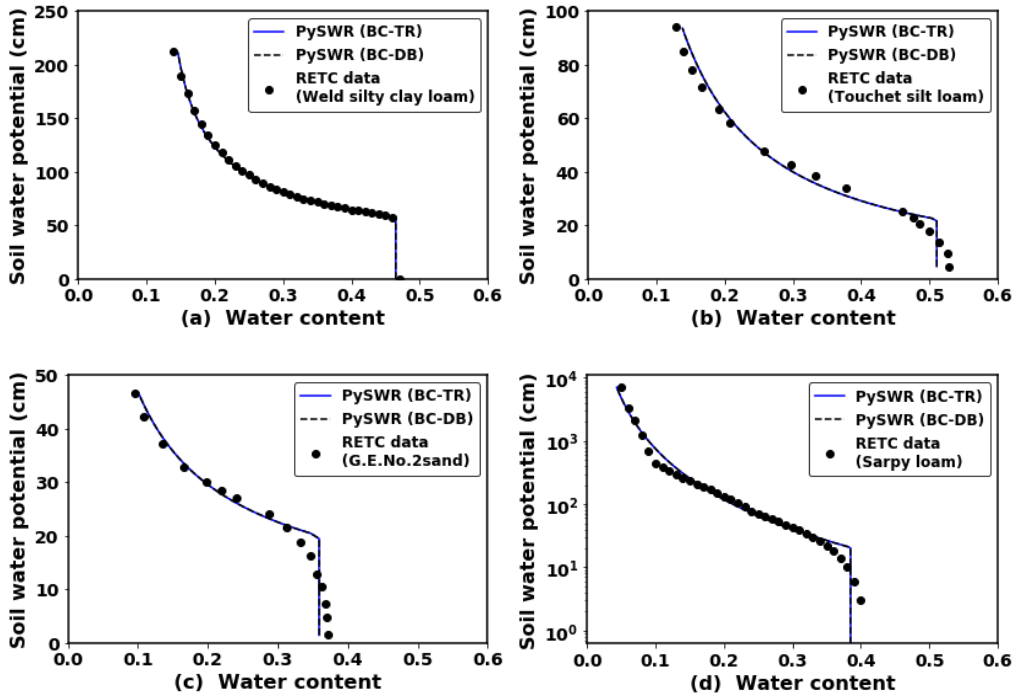
305 We employed the values given in Table 5 to fit the BC model to all four RETC soil datasets and  
 306 the results are shown in Figure 4.

307

308

309





310

311

312 **Figure 4.** Brooks and Corey model fit for the four RETC soils fitted using the TR and DB  
 313 methods: (a) Weld silty clay loam (Jensen and Hanks, 1967) (b) Touchet silt loam (King, 1965)  
 314 (c) G.E.No.2 sand (King, 1965) (d) Sarpy loam (Hanks and Bowers, 1962).

315

316 The results show that both TR and DB methods fitted the data well. In Table 6 we only provide  
 317 the TR results and compare them with the values estimated by the RETC code. These data show  
 318 that the model parameter estimated by PySWR are close to the RETC estimates. Also, the  
 319 estimated values of SSE in Table 6 indicate that the TR method performed similar or better when  
 320 compared to RETC code results, for all four datasets.

321

322

323

324 **Table 6.** The values of Brooks and Corey model parameters estimated by TR method for the four  
 325 RETC soils.

Soil type	Method	$\theta_r$	$\theta_s$	$\lambda$	$\alpha$ ( $\text{cm}^{-1}$ )	<b>SSE</b> ( $10^{-3}$ )
Weld silty clay loam (Jensen and Hanks, 1967)	TR	0.112±(0.003)	0.470±(0.003)	1.83±(0.03)	0.01739±(6e-5)	0.21
	RETC code	0.11	0.46	1.89	0.017	0.21
Toucher silt loam (King 1965)	TR	0.00	0.510±(0.007)	0.9±(0.2)	0.045±(1e-3)	2.25
	RETC code	0.018	0.499	1.1	0.037	3.67
G. E. No.2 sand (King, 1965)	TR	0.00	0.358±(0.004)	1.5±(0.5)	0.049±(1e-3)	1.56
	RETC code	0.00	0.352	1.7	0.046	3.54
Sarpy loam (Hanks and Bowers, 1962)	TR	0.00	0.380±(0.004)	0.38±(0.04)	0.044±(2e-3)	5.38
	RETC code	0.00	0.380	0.38	0.044	5.39

326

### 327 *3.3 Comparison of the efficiency of different non-linear fitting approaches*

328 To understand the relative efficiency of the three fitting approaches, we artificially perturbed the  
 329 Touchet silt loam (King, 1965) data (the perturbed dataset is given in Table S4, see  
 330 Supplementary Material) by introducing some random noise to the data. We employed the  
 331 graphical approach for reevaluating the initial guesses and parameter bounds for the noisy  
 332 dataset and the results are summarized in Table S5 (see Supplementary Material). We then used  
 333 all three methods to fit both VG and BC models to this noisy dataset. The estimated model  
 334 parameter values are summarized in Table 7; note, in the table we only report the values  
 335 estimated by TR because the LM method failed, and TR and DB methods generated similar  
 336 results. Figure 5 shows the model profiles fitted using the TR and DB methods. The figure  
 337 clearly shows that both TR and DB fits were almost identical. The most interesting result of this  
 338 efficiency test was that the LM method not only failed to fit the BC model (which should be  
 339 expected) but also failed to fit the VG model when the data was noisy.

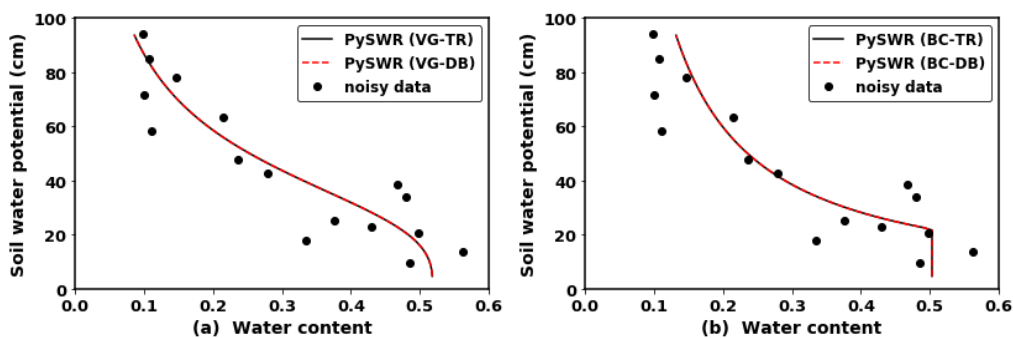
340 Our simulation results also indicated that for most cases the TR method is a bit more  
 341 computationally efficient than the DB approach (e.g., see Table 2). We completed additional  
 342 sensitivity simulations by perturbing the initial guess values; the results indicated that for some  
 343 soils the DB method can be relatively more sensitive to initial guess values when compared to  
 344 the TR method. Overall, we found the TR method as the most robust approach for fitting both  
 345 VG and BC models. Therefore, in the following validation section, we only present the results  
 346 for the TR method.

347 **Table 7.** The values of van Genuchten and Brooks and Corey model parameters  
 348 estimated for the noisy Touchet silt loam (King 1965) data (note, we only report TR  
 349 results since

Method	$\theta_r$	$\theta_s$	$n$ or $\lambda$	$\alpha$ or $\square$ ( $\text{cm}^{-1}$ )
VG-TR	0	$0.51 \pm (0.05)$	$3 \pm (2)$	$0.025 \pm (0.005)$
BC-TR	0	$0.50 \pm (0.04)$	$0.9 \pm (1)$	$0.045 \pm (0.008)$

350 LM failed to  
 351 and DB  
 352 were identical to TR).

353  
 354  
 355

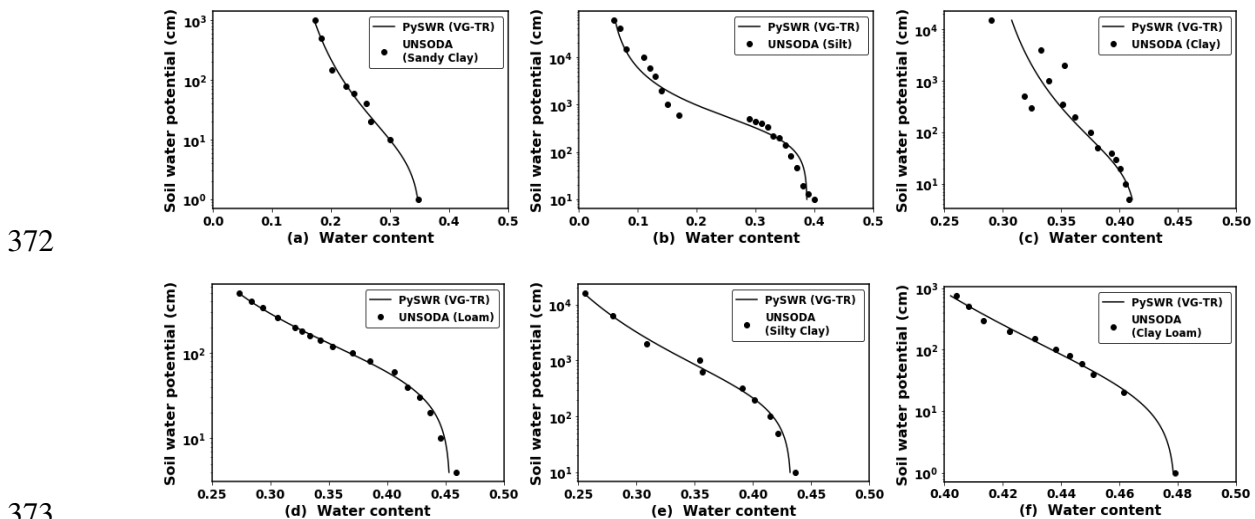


356 **Figure 5.** TR and DB fits for the noisy Touchet silt loam data (King, 1965): (a) van Genuchten  
 357 function model results and (b) Brooks and Corey model results.

359

### 360 3.4 Validation of the code performance using additional datasets

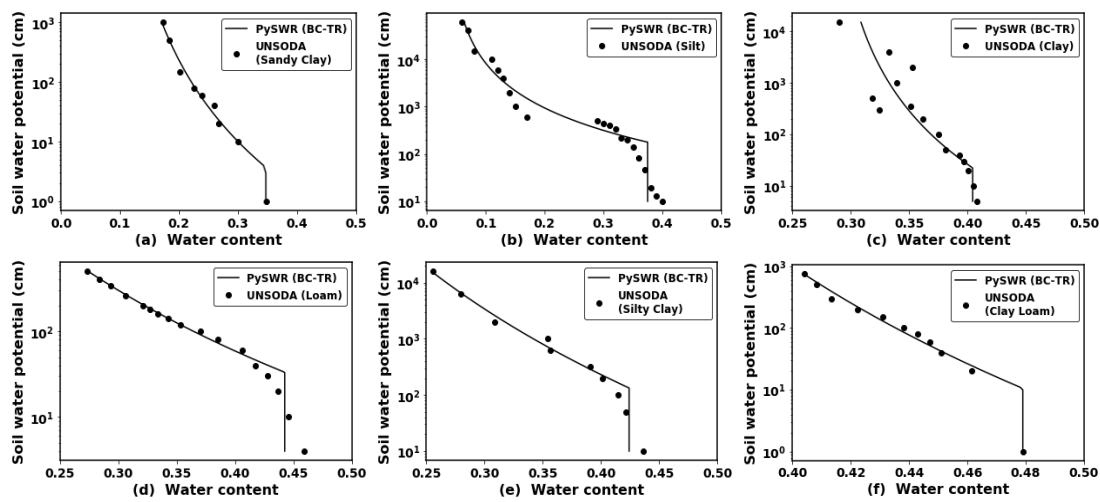
361 To further test the performance of the PySWR code, we used the code to fit both VG and BC  
 362 models to six different UNSODA datasets. We first analyzed these experimental data using the  
 363 proposed graphical approach and evaluated the initial guesses and bounding values for all the  
 364 model parameters. These values are summarized in Table S6 (see Supplementary Material).  
 365 We used the TR method to fit the VG model to the six UNSODA soils and the fitted model  
 366 profiles are compared with the experimental data in Figure 6. The figures show that the PySWR  
 367 code was able to fit all UNSODA datasets well. The estimated model parameter values are  
 368 compared against the SSA (Zhang et al., 2018) and RETC code results in Table S7 (see  
 369 Supplementary Material). From the values of SSE, summarized in Table S7 it can be observed  
 370 that the TR method was able to provide better fits with relatively low SSE values when  
 371 compared to RETC fits.



374 **Figure 6.** van Genuchten model fits for the six UNSODA soils fitted using the TR method: (a)  
 375 Sample 1102 (Sandy Clay), (b) Sample 1330 (Silt), (c) Sample 1162 (Clay), (d) Sample 2400  
 376 (Loam), (e) Sample 1361 (Silty Clay), (f) Sample 1173 (Clay Loam).

377

378 The TR method was then used to fit the BC model to all UNSODA soils. The model profiles  
 379 fitted by the PySWR code are compared with experimental data in Figure 7. The figure shows  
 380 that the TR method was able to fit the BC model to all six datasets. Furthermore, the fitted model  
 381 parameter values are summarized in Table S8 (see Supplementary Material). The values  
 382 presented in the table (see S8) show that the code was able to estimate realistic model  
 383 parameters.



384  
 385  
 386 **Figure 7.** Brooks and Corey model fit for six UNSODA soils fitted using the TR method: (a)  
 387 Sample 1102 (Sandy Clay), (b) Sample 1330 (Silt), (c) Sample 1162 (Clay), (d) Sample 2400  
 388 (Loam), (e) Sample 1361 (Silty Clay), and (f) Sample 1173 (Clay Loam).

389  
 390 As discussed in the aforementioned sections, unlike the VG model, the BC model is not a smooth  
 391 function and has a discontinuity close to the air-entry value. Comparisons of experimental data  
 392 shown in Figure 6 and Figure 7 indicate that the initial drainage pattern was fairly smooth for all  
 393 six UNSODA soils. As expected, the sharp transition region near the air entry value resulted in  
 394 the BC function not fitting some of the data points located near high water content values. The  
 395 VG model, which simulated a smoother drainage pattern provided better fits for all six  
 396 UNSODA datasets. Our test simulations indicated that for most of our cases, the VG model

397 performed well even when generic initial guesses and generic upper and lower bounds were  
398 used. On the other hand, the BC model required better initial values and narrower bounds to  
399 obtain meaningful results. Overall, the VG model was a better function for describing the  
400 UNSODA data.

#### 401 **4. Conclusions**

402 We present the details of a Python code, PySWR, for fitting VG and BC models to soil moisture  
403 data. PySWR provides options to use several non-linear least-squares fitting methods, including  
404 LM, TR, and DB methods, available in the Python SciPy module. The results show that all three  
405 methods were able to fit the VG model to the four RETC soil datasets. However, further analysis  
406 indicated that the LM method failed to fit the VG model when some random noise was  
407 introduced into the data. The LM method also failed to fit the BC model to all the experimental  
408 datasets considered in this study. The TR and DB methods were found to be much better  
409 alternatives since they allowed the user to constrain the bounds of various model parameters,  
410 thus limiting the search within a feasible range. The efficiency of these methods can be  
411 improved by providing good initial guesses, and better upper and lower parameter bounds. The  
412 graphical method proposed in this study is an intuitive practical approach for evaluating good  
413 guesstimates and parameter bounds. The performance of the DB method was always comparable  
414 to the TR method; however, we recommend the use of the TR method since it was relatively less  
415 sensitive to variations in initial guess values, and it was also a bit more computationally efficient  
416 than the DB method. Our results show that PySWR is an excellent tool for analyzing SWR data.  
417 The PySWR code has tools for estimating parameter error, and it also supports various plotting  
418 routines for comparing model-fitted SWR curves with experimental data. Overall, PySWR is a  
419 useful tool for fitting both VG and BC models to experimental data.

420

421

422 **Acknowledgment**

423 This work was, in part, supported by NOAA/UCAR under contract NA18NWS4620043B, and

424 NSF Award Number: 2019561. Both SSM and TPC co-wrote the manuscript and contributed

425 equally to this effort. We like to thank Computers & Geosciences journal reviewers for their

426 helpful review comments.

427 **Computer Code Availability**

428 The PySWR code was jointly developed by the authors and their contact details are given above.

429 The Python code was developed using the Spider interface and was tested on a Windows

430 computer with Intel (R) i5 processor and 8.00 GB memory. The code is available at

431 <https://github.com/tpclement/PySWR>.

432

433

434

435

436

437

438

439

440

441

442

443

444

445 **References**

- 446 Brooks, R.H. and Corey, A.T. 1964. Hydraulic properties of porous media and their relation to  
447 drainage design. Transactions of the ASAE 7(1), 26-0028.
- 448 Campbell, G.S. 1974. A simple method for determining unsaturated conductivity from moisture  
449 retention data. Soil science 117(6), 311-314.
- 450 Chen, G., Jiao, L. and Li, X. 2016. Sensitivity analysis and identification of parameters to the  
451 Van Genuchten equation. Journal of Chemistry 2016, 8.
- 452 Clement, T., Hooker, B. and Skeen, R. 1996. Macroscopic models for predicting changes in  
453 saturated porous media properties caused by microbial growth. Ground Water 34(5), 934-  
454 942.
- 455 Clement, T., Wise, W.R. and Molz, F.J. 1994. A physically based, two-dimensional, finite-  
456 difference algorithm for modeling variably saturated flow. Journal of Hydrology 161(1-  
457 4), 71-90.
- 458 Cornelis, W.M., Khlosi, M., Hartmann, R., Van Meirvenne, M. and De Vos, B. 2005.  
459 Comparison of unimodal analytical expressions for the soil-water retention curve. Soil  
460 Science Society of America Journal 69(6), 1902-1911.
- 461 Doherty, J.E., Hunt, R.J. and Tonkin, M.J. 2010. Approaches to highly parameterized inversion:  
462 A guide to using PEST for model-parameter and predictive-uncertainty analysis. US  
463 Geological Survey Scientific Investigations Report 5211, 71.
- 464 Fletcher, R. (1980) Practical Methods Of Optimization: Unconstrained Optimization, John Wiley  
465 & Sons.
- 466 Fredlund, D.G. and Xing, A. 1994. Equations for the soil-water characteristic curve. Canadian  
467 geotechnical journal 31(4), 521-532.
- 468 Fuentes, C., Haverkamp, R. and Parlange, J.-Y. 1992. Parameter constraints on closed-form  
469 soilwater relationships. Journal of hydrology 134(1-4), 117-142.
- 470 Gardner, W.R. 1958. Some steady state solutions of unsaturated moisture flow equations with  
471 application to evaporation from a water table. Soil Science 85(4), 228-232.
- 472 Guellouz, L., Askri, B., Jaffré, J. and Bouhlila, R. 2020. Estimation of the soil hydraulic  
473 properties from field data by solving an inverse problem. Scientific Reports 10(1), 1-11.
- 474 Hanks, R. and Bowers, S. 1962. Numerical solution of the moisture flow equation for  
475 infiltration into layered soils. Soil Science Society of America Journal 26(6), 530-534.



- 476 Jensen, M.E. and Hanks, R.J. 1967. Nonsteady-state drainage from porous media. Proceedings  
477 of the American Society of Civil Engineers, Journal of the Irrigation and Drainage  
478 Division 93(IR3), 209-231.
- 479 Ket, P., Oeurng, C. and Degré, A. 2018. Estimating Soil Water Retention Curve by Inverse  
480 Modelling from Combination of In Situ Dynamic Soil Water Content and Soil Potential  
481 Data. *Soil Systems* 2(4), 55.
- 482 King, L. 1965. Description of soil characteristics for partially saturated flow. *Soil Science  
483 Society of America Journal* 29(4), 359-362.
- 484 Kumar, N., Poddar, A. and Shankar, V. 2020. Nonlinear Regression for Identifying the Optimal  
485 Soil Hydraulic Model Parameters. 979, 25-34.
- 486 Lai, J. and Ren, L. 2016. Estimation of effective hydraulic parameters in heterogeneous soils at  
487 field scale. *Geoderma* 264, 28-41.
- 488 Le, T.M., Fatahi, B., Khabbaz, H. and Sun, W. 2017. Numerical optimization applying trust-  
489 region reflective least squares algorithm with constraints to optimize the non-linear creep  
490 parameters of soft soil. *Applied Mathematical Modelling* 41, 236-256.
- 491 Lenhard, B.R.J., Parker, J.C. and Mishra, S. 1989. On the correspondence between Brooks  
492 Corey and van Genuchten models. *Journal of Irrigation and Drainage Engineering*  
493 115(4), 744-751.
- 494 Levenberg, K. 1944. A method for the solution of certain non-linear problems in least squares.  
495 *Quarterly of applied mathematics* 2(2), 164-168.
- 496 Li, Y.B., Liu, Y., Nie, W.B. and Ma, X.Y. 2018. Inverse modeling of soil hydraulic parameters  
497 based on a hybrid of vector-evaluated genetic algorithm and particle swarm optimization.  
498 *Water* 10(1), 84.
- 499 Luo, X., Cao, L., Wang, L., Zhao, Z. and Huang, C. 2018. Parameter identification of the  
500 photovoltaic cell model with a hybrid Jaya-NM algorithm. *Optik* 171, 200-203.
- 501 Malaya, C. and Sreedeeep, S. 2012. Critical review on the parameters influencing soil-water  
502 characteristic curve. *Journal of Irrigation and Drainage Engineering* 138(1), 55-62.
- 503 Marquardt, D.W. 1963. An algorithm for least-squares estimation of nonlinear parameters.  
504 *Journal of the society for Industrial and Applied Mathematics* 11(2), 431-441.
- 505 Masaoka, N. and Kosugi, K.i. 2018. Improved evaporation method for the measurement of the  
506 hydraulic conductivity of unsaturated soil in the wet range. *Journal of Hydrology* 563,  
507 242-250.
- 508 Mohanty, B.P. and Zhu, J. 2007. Effective hydraulic parameters in horizontally and vertically  
509 heterogeneous soils for steady-state land-atmosphere interaction. *Journal of  
510 Hydrometeorology* 8(4), 715-729.

- 511 Nascimento, Í.V.d., Assis Júnior, R.N.d., Araújo, J.C.d., Alencar, T.L.d., Freire, A.G., Lobato,  
512 M.G.R., Silva, C.P.d., Mota, J.C.A. and Nascimento, C.D.V.d. 2018. Estimation of van  
513 Genuchten Equation Parameters in Laboratory and through Inverse Modeling with  
514 Hydrus-1D. *Journal of Agricultural Science* 10(3), 102.
- 515 Omuto, C. and Gumbe, L. 2009. Estimating water infiltration and retention characteristics using  
516 a computer program in R. *Computers & Geosciences* 35(3), 579-585.
- 517 Roy, D., Jia, X., Steele, D.D. and Lin, D. 2018. Development and Comparison of Soil Water  
518 Release Curves for Three Soils in the Red River Valley. *Soil Science Society of America  
519 Journal* 82(3), 568-577.
- 520 Schaap, A., Leij, M., Wösten, F.J. and M, J.H. 2015 UNSODA 2.0: Unsaturated Soil Hydraulic  
521 Database. Database and program for indirect methods of estimating unsaturated hydraulic  
522 properties.
- 523 Schindler, U., Mueller, L., da Veiga, M., Zhang, Y., Schlindwein, S. and Hu, C. 2012.  
524 Comparison of water-retention functions obtained from the extended evaporation method  
525 and the standard methods sand/kaolin boxes and pressure plate extractor. *Journal of Plant  
526 Nutrition and Soil Science* 175(4), 527-534.
- 527 Shin, Y., Mohanty, B.P. and Ines, A.V. 2012. Soil hydraulic properties in one-dimensional  
528 layered soil profile using layer-specific soil moisture assimilation scheme. *Water  
529 Resources Research* 48(6).
- 530 Shokrana, M.S.B. and Ghane, E. 2020. Measurement of soil water characteristic curve using  
531 HYPROP2. *MethodsX* 7, 100840.
- 532 Simunek, J. and Van Genuchten, M.T. 1999. Using the HYDRUS-1D and HYDRUS-2D codes  
533 for estimating unsaturated soil hydraulic and solute transport parameters.  
534 Characterization and measurement of the hydraulic properties of unsaturated porous  
535 media 1, 523-521.
- 536 Sorensen, D.C. 1982. Newton's method with a model trust region modification. *SIAM Journal  
537 on Numerical Analysis* 19(2), 409-426.
- 538 Stankovich, J. and Lockington, D. 1995. Brooks-Corey and van Genuchten soil-water-retention  
539 models. *Journal of Irrigation and drainage Engineering* 121(1), 1-7.
- 540 Tuller, M., Or, D. and Hillel, D. 2004. Retention of water in soil and the soil water  
541 characteristic curve. *Encyclopedia of Soils in the Environment* 4, 278-289.
- 542 Van Genuchten, M.T. 1980. A closed-form equation for predicting the hydraulic conductivity  
543 of unsaturated soils *Soil science society of America journal* 44(5), 892-898.
- 544 Van Genuchten, M.T. and Yates, F.J.L.a.S.R. 1991 The RETC Code for Quantifying the  
545 Hydraulic Functions of Unsaturated Soils.

- 546 Voglis, C. and Lagaris, I. 2004 A rectangular trust region dogleg approach for unconstrained  
547 and bound constrained nonlinear optimization.
- 548 Wang, J.-P., Hu, N., François, B. and Lambert, P. 2017. Estimating water retention curves and  
549 strength properties of unsaturated sandy soils from basic soil gradation parameters. *Water*  
550 *Resources Research* 53(7), 6069-6088.
- 551 Wang, T., Franz, T.E., Yue, W., Szilagyi, J., Zlotnik, V.A., You, J., Chen, X., Shulski, M.D. and  
552 Young, A. 2016. Feasibility analysis of using inverse modeling for estimating natural  
553 groundwater recharge from a large-scale soil moisture monitoring network. *Journal of*  
554 *Hydrology* 533, 250-265.
- 555 Wise, W.R. 1992. A new insight on pore structure and permeability. *Water Resources Research*  
556 28(1), 189-198.
- 557 Wise, W.R., Clement, T. and Molz, F.J. 1994. Variably saturated modeling of transient  
558 drainage: sensitivity to soil properties. *Journal of Hydrology* 161(1-4), 91-108.
- 559 Zhang, J., Wang, Z. and Luo, X. 2018. Parameter Estimation for Soil Water Retention Curve  
560 Using the Salp Swarm Algorithm. *Water* 10(6), 815.
- 561